Precipitation and the dimensional transition from weather to low frequency weather

Lovejoy, Shaun
McGill University, Physics department
3600 University st.
Montreal, H3A 2T8 Canada
Lovejoy@physics.mcgill.ca

Schertzer, Daniel
CEREVE, U. de Paris Est
77455 Marne-la-Vallee Cedex 2
France
Daniel.Schertzer@enpc.fr

1. Introduction

We have recently reviewed work on the emergent dynamical laws of multifractal cascade processes which are believed to hold in strongly turbulent fluids. For atmospheric dynamics, these laws provide a "new synthesis" of nonlinear theory and state of the art atmospheric data models and reanalyses, they are generalizations of the classical laws of turbulence to strongly anisotropic, strongly intermittent systems (Lovejoy and Schertzer, 2010). Such multifractal cascades provide accurate stochastic models of atmospheric fields – including precipitation – up to planetary scales. Since the lifetimes of planetary sized structures in the atmosphere are of the order of $\tau_w \approx 10$ days, (Lovejoy and Schertzer, 2011), the temporal scaling undergoes a drastic transition from a strongly variable high frequency "weather" regime where fluctuations in a field f varies as $\Delta f \approx \tau^H$ where τ is the time lag and H a scaling exponent. For $\tau<\tau_w$; the weather regime, we generally have $H>0$, for $\tau>\tau_w$, $H<0$ so that fluctuations no longer grow but diminish with scale. In spectral terms (and ignoring the intermittency correction $K(2)$, see below) we find $E(\omega) \approx \omega^{-\beta}$ with $\beta=1+2H$ so that at high frequencies $\omega>\omega_w = \tau_w^{-1}$, $\beta>1$ whereas at low frequencies $\omega<\omega_w = \tau_w^{-1}$, $\beta<1$ so that the spectra are much flatter: the resulting "low frequency weather" regimes have been called "spectral plateaus" (Lovejoy and Schertzer, 1986), see fig. 1 for an illustration with precipitation. For the oceans, the turbulent dynamics are very similar but $\tau_o \approx 1$ *yr*.

2 The fractionally Integrated Flux (FIF) model

The basic model which reproduces the weather regime cascade process is the Fractionally Integrated Flux model which is an explicit space-time stochastic cascade model. We first recall its basic features for the turbulent flux ε. First, since it is assumed to be a multiplicative process, it can be expressed in terms of the exponential of an additive generator Γ:

$$\varepsilon(\underline{r},t) = e^{\Gamma(\underline{r},t)} \qquad (1)$$

where Γ is the (dimensionless) generator and we have nondimensionalized ε by its ensemble average. If we assume that the basic statistics are translationally invariant in space-time (statistically homogeneous, statistically stationary), then Γ is given by a convolution between a basic noise $\gamma_\alpha(\underline{r},t)$ (independent, identically distributed random variables), and $g(\underline{r},t)$ is a Green's function "propagator" (a deterministic weighting function that correlates them over (potentially) large space-time distances):

$$\Gamma(\underline{r},t) = \gamma_\alpha(\underline{r},t) * g(\underline{r},t) \tag{2}$$

"*" indicates a space-time convolution over a finite range of scales λ; see below for more details. For the stable and attractive processes leading to universal multifractals, $\gamma_\alpha(\underline{r},t)$ is taken as a unit (and extremal) Levy noise, index α, i.e. whose second characteristic function is $K_\gamma(q) = \log\left\langle e^{\gamma_\alpha q}\right\rangle = q^\alpha/(\alpha-1)$ where "< >" means ensemble averaging. Due to the additivity of the second characteristic functions this yields:

$$\log\left\langle \varepsilon_\lambda^q \right\rangle = \log\left\langle e^{q\Gamma}\right\rangle = \frac{1}{\alpha-1}\int_{s_\lambda} g^\alpha d\underline{r}\,dt \tag{3}$$

where s_λ is the domain of integration of the convolution, over a range of scales factor λ; see below. In addition, for universal multifractals, g must have a particular form:

$$g(\underline{r},t) = N_D C_1^{1/\alpha}\Theta(t)\left[\!\left[(\underline{r},t)\right]\!\right]^{-D/\alpha} \tag{4}$$

with the singularity cutoff at the inner, dissipation scale and the dimension of space-time $D = d+1$ where d is the number of spatial dimensions, N_D is a normalization constant, C_1 the intermittency parameter of the mean intermittency, α is the Levy index of the Levy noise $\gamma_\alpha(\underline{r},t)$, $\left[\!\left[(\underline{r},t)\right]\!\right]$ is the space-time scale function which is analogous to the vector norm and which characterizes the space-time scale. See (Schertzer and Lovejoy, 1987) for the basic model, (Marsan et al., 1996) for the extension to causal space-time processes, (Lovejoy et al., 2008) for the extension to turbulence driven waves, and (Lovejoy and Schertzer, 2009) for a technical treatment of numerical issues. Causality has been taken into account with the use of a Heaviside function Θ(t) (=0 for $t<0$, = 1 for $t>0$), (Marsan et al., 1996). Physically, the noise γ_α represents the innovations and g the interaction strength. If the convolution is taken over a scale range λ, (e.g. $\lambda^{-1} < \left[\!\left[(\underline{r},t)\right]\!\right] < 1$) then eqs. 2-4 together imply the logarithmic divergence of the integral in eq. 3, hence the multifractal scaling of the flux:

$$\left\langle \varepsilon_\lambda^q \right\rangle = \lambda^{K(q)};\quad K(q) = \frac{C_1}{\alpha-1}\left(q^\alpha - q\right) \tag{5}$$

(the linear term results from normalizing: $\varepsilon_\lambda \to \varepsilon_\lambda / \left\langle \varepsilon_\lambda \right\rangle$). Figure 2 shows data analyses of

gauge, satellite radar and reanalysis data indicating that eq. 5 holds accurately for large scale rain fluxes. The observable R (e.g. the rain rate) whose fluctuation (ΔR) statistics obey $\left\langle |\Delta R|^q \right\rangle \approx [\![(\underline{\Delta r}, \Delta t)]\!]^{\xi(q)}$ where $\xi(q) = qH - K(q)$ can be obtained from the flux by taking:

$$R(\underline{r},t) = \varepsilon(\underline{r},t) * \left(\Theta(t)[\![(\underline{r},t)]\!]\right)^{-(D-H)} \tag{6}$$

Eqs. 1-4 are the causal space-time extension of the "Fractionally Integrated Flux" (FIF) model for the turbulent flux, and eq. 6 for the field R, (Schertzer and Lovejoy, 1987).

In order to understand the basic model features we can restrict our attention to the horizontal D=2+1, (x, y, t) section of the full (x, y, z, t) model and ignore the complications associated with ocean augmented intermittency. If we rewrite the equation for the cascade generator nondimensionalizing x, y with L_e (= 20,000 *km*; the subscript "*e*" for "earth") and t with τ_w, we obtain explicitly for the generator $\Gamma(\underline{r},t) = \log \varepsilon(\underline{r},t)$:

$$\Gamma(\underline{r},t) = \int_{\Lambda_w^{-1}}^{1} \int_{s_w} \gamma(\underline{r}-\underline{r}', t-t') g(\underline{r}', t') d\underline{r}' dt' + \int_{1}^{\Lambda_c} \int_{s_w} \gamma(\underline{r}-\underline{r}', t-t') g(\underline{r}', t') d\underline{r}' dt' \tag{7}$$

$\Lambda_w = L_w / L_i = \tau_w / \tau_i$ is the total range of meteorological scales (L_i, τ_i are the inner, dissipation space and time scales) and $\Lambda_c = \tau_c / \tau_w$ is the ratio of the overall outer time scale τ_c of the low frequency weather process marking the beginning of a new (very) low frequency "climate" regime and s_w is the spatial domain of integration in these nondimensional coordinates, from Λ_w^{-1} to 1). Eq. 7 is a convolution between the subgenerator noise γ which represents the "innovations" and the power law kernel g represents the interaction strength between scales physically and temporally separated by the space-time interval ($\underline{r}'$, t'). For $\Lambda_c = \tau_c/\tau_w >> 1$ we therefore have approximately:

$$\begin{aligned} \Gamma(\underline{r},t) &\approx \Gamma_w(\underline{r},t) + \Gamma_{lw}(t) \\ \Gamma_w(\underline{r},t) &= \int_{\Lambda_w^{-1}}^{1} \int_{S_w} \gamma\left(\underline{r}-\underline{r}', t-t'\right) g\left(\underline{r}', t'\right) d\underline{r}' dt' \\ \Gamma_{lw}(t) &= \int_{1}^{\Lambda_c} \overline{\gamma}(t-t') g(0,t') dt' \end{aligned} \tag{8}$$

where $\overline{\gamma}(t-t')$ is a spatially integrated Lévy noise. The region of integration in the weather integral s_w can be approximated by the quarter unit circle in $\underline{r}$ = (x,y) space with the quarter circle around the origin of radius Λ_w^{-1} removed. The approximation in eq. 8 consists in assuming for $t >> |\underline{r}|$ that $g(x,y,t) \approx g(0,0,t)$ so that for long enough time lags the spatial lags are unimportant. $\Gamma_w(\underline{r},t)$ is a 3 D integral corresponding to the contribution to the variability from the weather regime ($t < 1$, $|\underline{r}| < 1$), and the second $\Gamma_{lw}(t)$ is a 1 D (purely)

temporal contribution due to the low frequency weather regime. This drastic change of behaviour due to the change of space –time dimension over which the basic noise driving the system acts is a kind of "dimensional transition" between the usual (high frequency) "weather" and "low frequency weather" processes. At small scales, the interactions occur over all spatial and temporal intervals (the interaction region is a space-time volume), whereas for long times, the interaction region is pencil-like, it is essentially 1-D. Physically this is a transition from the high frequency regime where both spatial and temporal interactions are important, to a lower frequency regime where the dynamics are dominated by temporal interactions. In the former case, this means between neighbouring structures of all sizes and at their various stages of development whereas in the latter case, only between very large structures at various stages in their development.

In this model it is this separation into independent additive weather and low frequency weather terms with correlated noises integrated over spaces of different effective dimensions which is responsible for the statistical difference between weather and low frequency weather plateau. At the level of the fluxes it means that the low frequency weather process multiplicatively modulates the weather process at the larger time scales:

$$\varepsilon_{\Lambda_w,\Lambda_c}(x,t) \approx e^{\Gamma_w(x,t)+\Gamma_{lw}(x,t)} = \varepsilon_{\Lambda_w}(x,t)\varepsilon_{\Lambda_c}(t) \qquad (9)$$

with $\varepsilon_{\Lambda_w}(\underline{r},t)$, having the high frequency variability, $\varepsilon_{\Lambda_c}(t)$ the low frequency. The generic result is a "dimensional transition" in the form of a fairly realistic spectral plateau (see fig. 1).

Let us assume that except for the causal restriction, that the propagator g is isotropic in (x,y,t) space so that for $\underline{r} = (x,y)$, $d = 2$ spatial dimension and time, nondimensionalizing x with L_w, and t with τ_w we have:

$$g(\underline{r},t) = \Theta(t)\left[\!\left[(\underline{r},t)\right]\!\right]^{-(d+1)/\alpha} = \Theta(t)\left(|\underline{r}|^2 + t^2\right)^{-1/\alpha} \qquad (10)$$

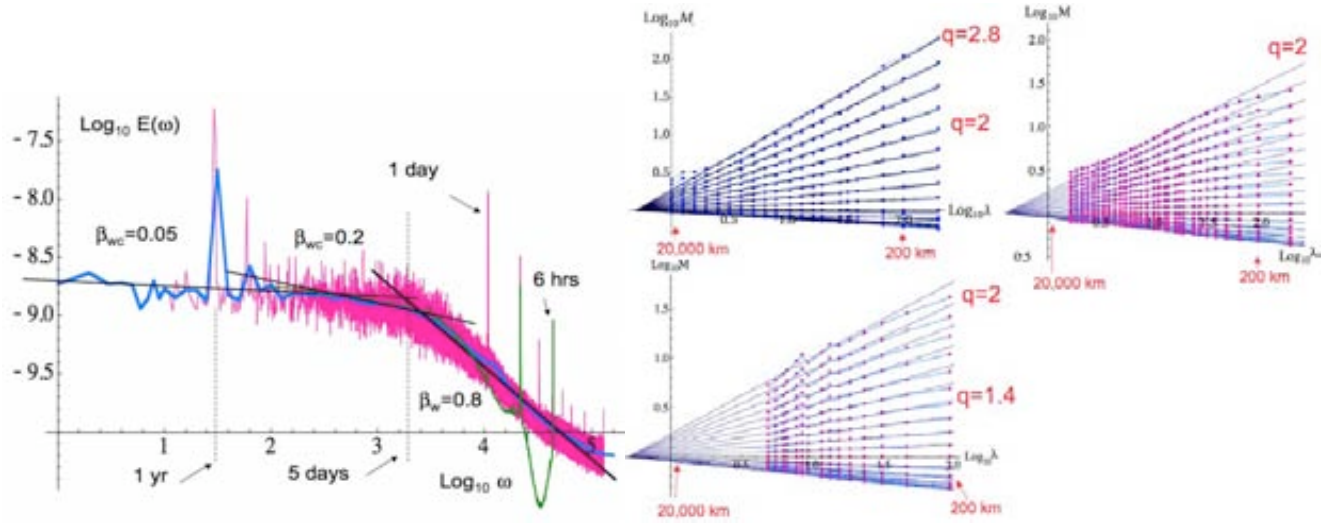

Figure 1 (left): A comparison of the temporal spectra of the CPC, continental US, hourly data grid on a ≈ 200x200 km grid (red) and the ECMWF interim reanalysis 1.5°, 3 hourly data set (green). The blue curve is the CPC spectrum averaged over logarithmically spaced

frequency bins (10 per order of magnitude). The transition scale from the high frequency weather regime and low frequency weather-climate regime is indicated by the dashed line at periods of 5 days. The axis is in units such that ω = 1 is (29 *yrs*)$^{-1}$; i.e. the full length of the CPC series. There are three reference lines with absolute slopes indicated. The low frequency weather has $\beta_{lw} \approx 0.05$, the high frequency weather regime, ≈ 0.8.

Figure 2 (right): East-west analyses of the gridded precipitation products discussed in the text. The normalized moments $M = \langle \varepsilon_\lambda^q \rangle / \langle \varepsilon_\lambda \rangle^q$ follow the regression lines (eq. 5), the slopes are $K(q)$ and they "point" to the effective outer scale (where the cascade effectively starts: $\lambda = L_e/L$, L_e =20000 *km*, L is the resolution). **Upper left:** The TRMM (radar satellite) 100x100 *km*, 4 day averaged product. **Upper right:** The ECMWF interim reanalysis stratiform rain product (all latitudes were used). Note that the data were degraded in constant angle bins so that the outer scale is 180°. To compare with the other analyses, a mean map factor of 0.69 has been applied (the mean east-west outer scale was ≈14,000 *km*). Lower left: The CPC hourly gridded rainfall product (US only). Reproduced from (Lovejoy et al., 2010). The fluxes were estimated by the absolute second differences in time. Empirically, from $K(q)$, we find $C_1 \approx 0.4$, $\alpha \approx 1.5$.

In d spatial dimensions, from eq. 8, we see that the weather-climate generator is:

$$\varepsilon_{lw}(t) = e^{\Gamma_{lw}(t)}; \quad \Gamma_{lw} = \left(\frac{C_1}{N_{d+1}} \right)^{1/\alpha} \gamma_\alpha * g_{lw}; \quad g_{lw} = \Theta(t) t^{-(d+1)/\alpha} \tag{11}$$

(N_{d+1} is a normalization constant) and this falls off more rapidly than for a d = 0 (pure temporal multifractal) cascade process (which requires $t^{-1/\alpha}$), leading to low intermittency.

3. The basic bare, dressed statistical behaviour in the spectral plateau

We now discuss the surprising statistics in the plateau regime: that although the statistical properties are indeed asymptotical scaling (power laws), that the actual "effective" exponent can depend on the cascade scale range – and yet be fairly accurately scaling over two to three orders of magnitude, i.e. physically, from $\tau_w \approx 10$ days to $\tau_c \approx 10$ years or more.

We have already seen in eq. 7 that the generator for the flux separates into the sum of a weather and climate contribution corresponding to the multiplicative modulation of the weather flux by a climate flux. If we nondimensionalize time by the weather scale τ_w we find that for scales $t = \lambda >> 1$, we can ignore the spatial degrees of freedom and the second characteristic function of the bare flux low frequency weather ε_λ is given by:

$$K_{lw}(q) = \log \langle \varepsilon_{lw,\lambda}^q \rangle = \frac{C_1 q^\alpha}{\alpha - 1} N_{d+1}^{-1} \int_{\Lambda_c/\lambda}^{\Lambda_c} \frac{dt}{t^{(1+d)}} = \frac{C_1 q^\alpha}{N_{d+1} d(\alpha - 1)} \Lambda_c^{-d} \left(\lambda^d - 1 \right) \tag{12}$$

where we have used the propagator eq. 11. This gives $g(0,t)^\alpha = \Theta(t) t^{-2}$ (d =1 spatial

dimension), $g(0,0,t)^{\alpha} = \Theta(t)t^{-3}$ (d =2 spatial dimensions), N_{d+1} is the causal normalization constant in d+1 dimensions: =2π/2 in d =1, 4π/2 in d =2 the factor 2 is due to the Heaviside function) note that the logarithms are taken to the base e rather than the base λ as in the usual cascade regime (which is recovered if we take d =0 in the above and replace the power laws by logarithms on the right). The above bare non-normalized function can be normalized by taking $\varepsilon_\lambda \to \varepsilon_\lambda / \langle \varepsilon_\lambda \rangle$ $K(q)->K(q)-qK(q)$, i.e. we replace q^α by $q^\alpha-q$ in eq. 12. Since $C_1<d+1$, the exponent $K_{lw}(q)$ is typically quite small so that the exponentiation needed to obtain $\langle \varepsilon_{lw,\lambda}^q \rangle$ yields:

$$\left\langle \varepsilon_{lw,\lambda}^q \right\rangle \approx 1 + K_{lw}(q) = 1 + \frac{C_1\left(q^\alpha - q\right)}{N_{d+1} d(\alpha - 1)} \Lambda_c^{-d}\left(\lambda^d - 1\right) \tag{13}$$

We thus see that the moments depend only weakly on C_1, q, λ. In any case, as usual, it is the dressed properties that are most important, and due to the weak correlations (studied explicitly below) we in fact fairly quickly obtain convergence to the (usual) Gaussian central limit theorem.

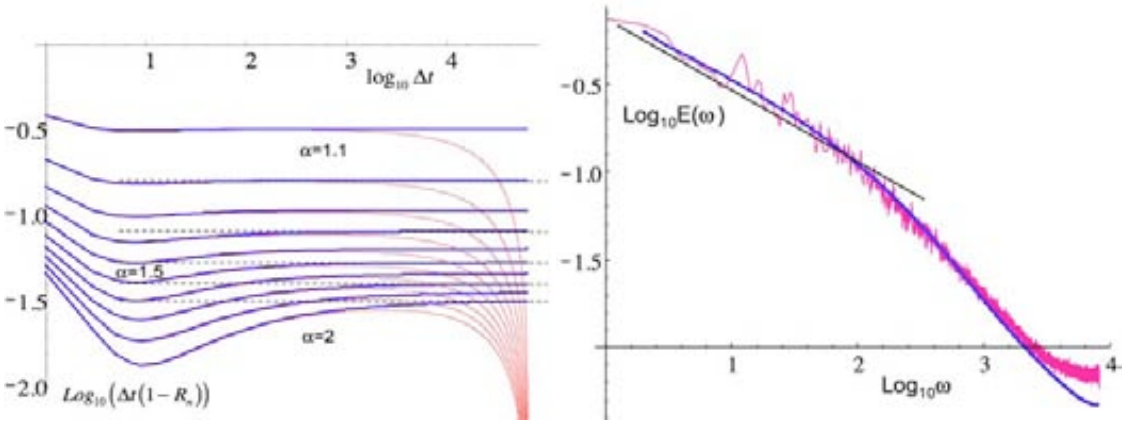

Figure 3 (left): The log of the compensated, normalized autocorrelation function in two spatial dimensions for C_1 = 0.4, the thick blue lines are when R_n is estimated using $R_n(\Delta t) = R(\Delta t)/R(\infty)$, the thin red lines are for $R_n(\Delta t) = R(\Delta t)/R(\Lambda_c)$ (important for the power spectrum over a finite range) and the dashed black lines are flat reference lines corresponding to the asymptotic Δt^{-1} behaviour. Λ_c = 2^{16}, showing the extreme sensitivity of the large scales to the length of the series (Λ_c). Each curve is for a different a value, increasing from 2 (bottom) to 1.1 (top) at intervals of 0.1.

Figure 4 (right): This compares Monte Carlo results for 40 realizations α = 1.8, C_1=0.1, 2^{14}x2^6 (time, space) with the corresponding theory (solid line) for one spatial dimension. For $\omega > 2^{14}/2^6 = 2^8$, (i.e. the transition is expected at $\log_{10}\omega \approx 2.4$) there is some disagreement since the spatial degrees of freedom (neglected for the solid line) begin to be important. The solid black reference line has a slope −0.4 which holds well for a factor of 100 or so in scale.

4. Autocorrelations: asymptotic Δt^{-1} scaling

In order to better understand the scale dependence of the plateau cascades, let us determine the autocorrelation function, from which the spectrum can be found by Fourier transformation (the Wiener–Khintchin theorem). In particular, considering just the low frequency weather regime, in nondimensional coordinates, after integrating out the small scale spatial degrees of freedom we obtain:

$$\log\left\langle \left(\varepsilon_\lambda(t)\varepsilon_\lambda(t-\Delta t)\right)^q \right\rangle = \log\left\langle e^{q(\Gamma(t)+\Gamma(t-\Delta t))} \right\rangle = \frac{C_1}{\alpha-1} q^\alpha S(\Delta t) \qquad (14)$$

the entire expression is the full Second Characteristic Function of the log of the autocorrelation, the key function $S(\Delta t)$ is its temporal part:

$$S(\Delta t) \approx \int_1^{\Lambda_c} \left(g(t)+g(t-\Delta t)\right)^\alpha dt; \qquad \begin{aligned} g(t) &= t^{-(d+1)/\alpha}; \quad t \geq 1 \\ g(t) &= 0; \qquad t < 1 \end{aligned} \qquad (15)$$

(this takes into account causality and is only the low frequency weather contribution, it ignores the weather scales $0<t<1$). Recall the normalized autocorrelation function $R_n(\Delta t)$:

$$R_n(\Delta t) = R(\Delta t)/R(\Lambda_c); \quad R(\Delta t) = e^{\frac{C_1}{\alpha-1} N_d^{-1} S(\Delta t)} \qquad (16)$$

Considering just the $d=1$ case for the moment, this yields:

$$S(\Delta t) \approx \int_1^{\Delta t-1} \frac{dt}{t^2} + \int_{\Delta t+1}^{\Lambda_c} \left(\frac{1}{t^{2/\alpha}} + \frac{1}{(t-\Delta t)^{2/\alpha}} \right)^\alpha dt \qquad (17)$$

This yields:

$$S(\Delta t) \approx 1 - \Delta t^{-1} + \Delta t^{-1} \int_{(1+\Delta t)^{-1}}^{(1+\Delta t/\Lambda_c)^{-1}} \frac{dr}{r^2} \left(1 + r^{2/\alpha}\right)^\alpha dr \qquad (18)$$

where we have used the transformation of variables:

$$r = \frac{t-\Delta t}{t}; \quad \frac{dt}{t^2} = \frac{dr}{\Delta t} \qquad (19)$$

Since there is no singularity at $r=1$, we can take Λ_c large, to high accuracy, we can take the upper bound as $r = 1$. We thus rewrite the integral as:

$$S(\Delta t) \approx 1 - \Delta t^{-1} + \Delta t^{-1} \left[\begin{aligned} &\int_0^1 \frac{dr}{r^2} \left(\left(1 + r^{2/\alpha}\right)^\alpha - 1 \right) dr \\ &- \int_0^{\Delta t^{-1}} \frac{dr}{r^2} \left(\left(1 + r^{2/\alpha}\right)^\alpha - 1 \right) dr + \int_{\Delta t^{-1}}^1 \frac{dr}{r^2} \end{aligned} \right] \qquad (20)$$

For $\alpha<2$, the first term in the brackets is a simple α dependent constant:

$$A = \int_0^1 \frac{dr}{r^2}\left(\left(1+r^{2/\alpha}\right)^{\alpha} - 1\right)dr \tag{21}$$

(e.g. A =16.379 for α =1.8), the third term is simply $\Delta t-1$ while the second term can be evaluated by using the binomial expansion yielding:

$$S(\Delta t) \approx 2 + (A-2)\Delta t^{-1} - \frac{\alpha}{2/\alpha - 1}\Delta t^{-2/\alpha} - O\left(\Delta t^{-4/\alpha}\right) \tag{22}$$

Just the first three terms yield an excellent approximation. Although the derivation is more involved, the more realistic case d = 2, also yields a Δt^{-1} asymptotic behavior. Since $(S(\Delta t) - S(\infty))_{<<1}$, we may use the approximation:

$$\frac{R(\Delta t)}{R(\infty)} = e^{\frac{C_1}{\alpha-1}N_{d+1}^{-1}(S(\Delta t)-S(\infty))} \approx 1 + \frac{C_1}{\alpha-1}N_{d+1}^{-1}\left(S(\Delta t) - S(\infty)\right) \tag{23}$$

we may thus numerically determine the range of Δt^{-1} behaviour by using the autocorrelation function normalized by the limiting value as $\Delta t \to \infty$. This relation (compensated by multiplying it by Δt) is confirmed in fig. 3 (thick lines) using direct numerical integration of the corresponding equation for d =2. Convergence to the theoretical asymptotic behaviour is very slow, especially for the larger α values. However, the situation is actually worse than this slow convergence indicates since for finite Λ_c, it is not the autocorrelation function normalized by $R(\infty)$ that is important, but rather (as in eq. 16) by $R(\Lambda_c)$, the largest in the cascade regime, and due to the extremely slow fall-off implied by the Δt^{-1} behaviour, this significantly modifies the large Δt behaviour as shown by the thin lines in Fig. 3. Due to this additional large Δt effect, the pure Δt^{-1} scaling only occurs at very large Δt (recall that even being generous, that empirically $\Lambda_c \approx <2^{12}$ (≈100 years/10 days).

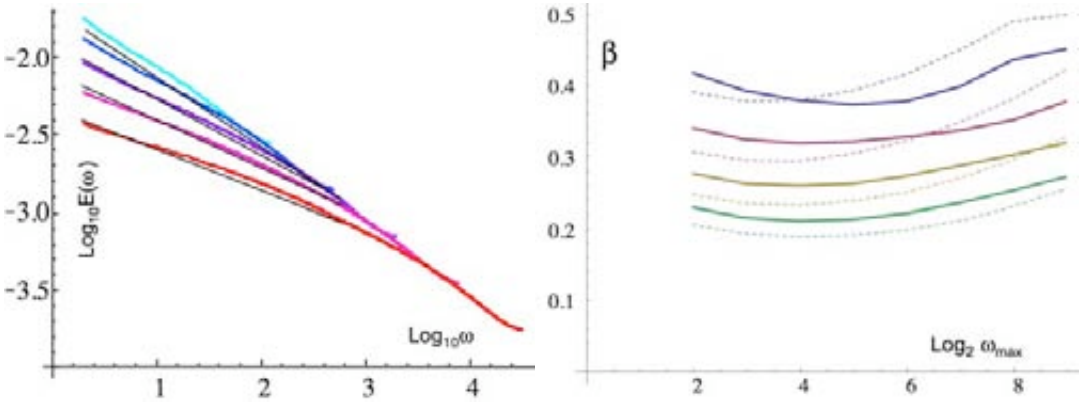

Figure 5 (left): The theoretical plateau power spectrum for α =1.8, two spatial dimensions (d = 2) for outer scales of 2^8, 2^{10}, 2^{12}, 2^{14}, 2^{16} (top to bottom). The lines have root mean square slopes fit up for $\omega \leq 512$, with values -0.45, -0.38, -0.32, -0.27 (the 2^8 line is not given since the corresponding simulation isn't long enough; see the next graph for a quantification).

Figure 6 (right): This shows the regression estimates of the spectral exponent β (the

absolute logarithmic slope) with fits from $\omega = 4$ to $\omega = \omega_{max}$, the latter increasing from left to right in two spatial dimensions ($d = 2$). The lines from top to bottom are for outer scales Λ_c increasing from 2^{10}, 2^{12}, 2^{14}, 2^{16}. The solid lines are for $\alpha = 1.8$, the dashed lines for $\alpha = 1.5$, all for two spatial dimensions. Over all the regression ranges, the standard deviations of the residuals are between ±0.008 and ±0.014 ($\alpha = 1.8$) and ±0.011 to ±0.019 ($\alpha = 1.5$).

5. Spectra, pseudo-scaling

We have seen that the asymptotic autocorrelation function has rather slow convergence to a Δt^{-1} form; for the spectrum (the Fourier transform), this is particularly problematic since the spectrum of a pure Δt^{-1} function diverges at both low wavenumbers (also in fact at high wavenumbers, but this is not relevant here). We may therefore anticipate that the actual spectrum will be quite sensitive to the outer scale limit Λ_c. To investigate this, we studied both MonteCarlo simulations (40 realizations of a multifractal in one spatial dimension and time), and the corresponding ensemble spectrum $E(\omega)$ obtained numerically for a simulation length $\Lambda_c = 2^{12}$, see fig. 4. From the figure, there are three key points to note. First, that the simulation and theoretical ensemble average spectrum calculated numerically from eq. 18 agree extremely well. Second, that over a remarkably wide range – a factor ≈ 100– 1000 – that the spectrum is nearly linear on a log-log plot, i.e. it is "nearly" a power law, it is easy to see that this behaviour could easily be mistaken for a real scaling regime. Third, that this $d = 1$ exponent is low (here, $\beta \approx 0.4$) and close to the values found empirically ($\beta \approx 0.2 - 0.4$, see (Lovejoy and Schertzer, 2011)), although precipitation is a little lower, see e.g. Fig. 1.

Returning to two spatial dimensions and calculating the ensemble averaged spectra directly numerically for various Λ_c, we obtain fig. 5. We can see that for the example given with $\alpha = 1.8$, that the apparently scaling low frequency regime is again of length a factor 100 – 1000 depending on how stringent we are about the linearity of the log-log spectrum (since S is small, virtually identical spectra are found for other values of C_1). Since the scaling regime is only approximate, it could be called "pseudo-scaling".

In the figure we also see that the pseudo scaling of the first factor 100 – 1000 depends to some extent on Λ_c as well as the maximum frequency (ω_{max}) used for the regression. In order to quantify this, we show in fig. 6 the regression β estimates as functions of ω_{max} for various Λ_c, and for $\alpha = 1.5$, 1.8 (the main empirical range). It can be seen that for ω_{max} between 4 and 512, the slopes are typically constant to ±0.05 and the standard deviations of the residuals of the fits are all <0.019. At the same time, β is a weak function of Λ_c; β changes by roughly 0.1 for every factor of 16 in Λ_c. We also note that taking $\Lambda_c \approx 100 - 300$ years/10 days $\approx 2^{12} - 2^{14}$ β is in the commonly range 0.2 – 0.4.

The final piece in the puzzle is to consider the plateau for the observables, the fractionally integrated fields (eq. 6). It turns out that the low frequency weather contribution to the fractional integration (i.e. the contribution for $t > 1$) is totally unimportant (see fig. 7). The reason is that fractional integration order H for the observable R_{lw}: $R_{lw}(t) = \Theta(t)\varepsilon_{lw}(t) * t^{-(d+1-H)}$

has essentially no effect on the spectrum since when $d - H > 0$, the one dimensional Fourier transform of $t^{-(d+1-H)}$ does not converge at small t so that $t^{-(d+1-H)}$ truncated at $t = 1$ is completely dominated by the truncation scale details.

In summary, we obtain spectra which are very nearly scaling over two to three orders of magnitude in scale whose exponents are independent of C_1, H, only weakly dependent on α and weakly dependent on the overall range of scales of the regime (Λ_c).

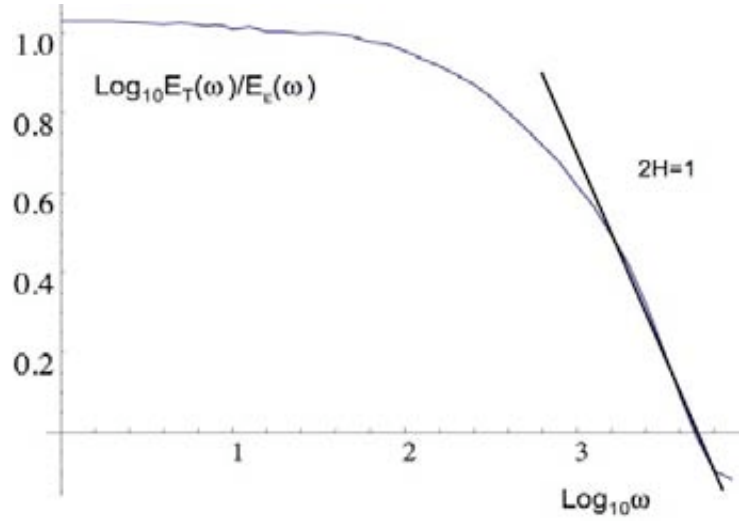

Figure 7: Using the same Monte Carlo realizations as in fig.4, we show the ratio of the spectra of the fractionally integrated precipitation field (E_T) (which was obtained by fractionally integrating, order H =1/2) the spectrum E_ε of the corresponding flux ε over 40 realizations (eq. 6). Since the (single) spatial dimension was 2^6 (compared to 2^{14} for time), the transition scale is $\omega_w = 2^8$ (note, $\log_{10}2^8 = 2.4$). We see that for the low frequencies, the fractional integration is totally ineffective; the ratio is constant.

7. REFERENCES

S. Lovejoy, J. Pinel and D. Schertzer, The Global space-time Cascade structure of precipitation: satellites, gauges and reanalyses, *Advances in Water Resources* (submitted 11/11)(2010).

S. Lovejoy and D. Schertzer, Scale invariance in climatological temperatures and the spectral plateau, *Annales Geophysicae* 4B(1986), pp. 401-410.

S. Lovejoy and D. Schertzer, On the simulation of continuous in scale universal multifractals, part I: spatially continuous processes, *Computers and Geoscience*(2009).

S. Lovejoy and D. Schertzer, Towards a new synthesis for atmospheric dynamics: space-time cascades, *Atmos. Res.* 96(2010), pp. pp. 1-52, doi:10.1016/j.atmosres.2010.1001.1004.

S. Lovejoy and D. Schertzer, The emergence of the Climate. In: A.S. Sharma, A. Bunde, D. Baker and V.P. Dimri, Editors, *Complexity and Extreme Events in Geosciences*, AGU monographs (2011).

S. Lovejoy, D. Schertzer, M. Lilley, K.B. Strawbridge and A. Radkevitch, Scaling turbulent atmospheric stratification, Part I: turbulence and waves, *Quart. J. Roy. Meteor. Soc.*(2008), p. DOI: 10.1002/qj.1201.

D. Marsan, D. Schertzer and S. Lovejoy, Causal space-time multifractal processes: predictability and forecasting of rain fields, *J. Geophy. Res.* 31D(1996), pp. 26,333-326,346.

D. Schertzer and S. Lovejoy, Physical modeling and Analysis of Rain and Clouds by Anisotropic Scaling of Multiplicative Processes, *Journal of Geophysical Research* 92(1987), pp. 9693-9714.